Decomposition of β-Hydroxypropoxy Radicals in the OH-Initiated Oxidation of Propene. A Theoretical and Experimental Study

Luc Vereecken and Jozef Peeters*,†

Department of Chemistry, University of Leuven, Celestijnenlaan 200F, B-3001 Leuven, Belgium

John J. Orlando*,‡ and Geoffrey S. Tyndall

Atmospheric Chemistry Division, National Center for Atmospheric Research, Boulder, Colorado 80303

Corinne Ferronato

Groupe de Recherche sur L'Environnement et la Chimie Appliquée (GRECA), Université Joseph Fourier, F-38000 Grenoble, France

Received: January 5, 1999; In Final Form: April 12, 1999

Environmental chamber studies of the OH-initiated oxidation of propene have been carried out in the presence of nitrogen oxides under conditions relevant to the atmosphere. The major products observed at all temperatures studied (220−300 K) are CH_2O and CH_3CHO, indicating that the β-hydroxypropoxy radicals formed in the oxidation process (from reaction of the corresponding β-hydroxypropylperoxy radicals with NO) predominantly undergo unimolecular decomposition. A full theoretical study of the chemistry of the dominant β-hydroxypropylperoxy, β-hydroxypropylperoxynitrite, and β-hydroxypropoxy species has been carried out. On the basis of B3LYP-DFT/6-31G** quantum chemical characterizations, the most stable conformations of the oxy radicals are found to contain intramolecular hydrogen bonds, which provide stabilizations of about 2 kcal/mol. The internal hydrogen bond in the lowest-energy oxy species is found to persist in the transition states for C−C bond rupture, which keeps the barrier to their decomposition down to 7.2 kcal/mol. By use of SSE theory, the internal energy distribution of the nascent $HOCH_2CH(O)CH_3$ oxy radicals has been determined; it is found that most radicals are born with internal energies well above the calculated barrier for their decomposition. Thus, as determined by master equation analysis, the majority of these oxy radicals (80% at 300 K and 1 atm, 75% at 220 K and 0.2 atm) will decompose promptly before collisional stabilization, yielding CH_2OH and CH_3CHO, while the remainder are thermalized. The rate coefficient of the thermal dissociation of $HOCH_2CH(O)CH_3$ was also theoretically evaluated; the results at 1 atm in the 220−300 K range can be expressed as $k_\infty = 3.5 \times 10^{13} \exp(-7.91 \text{ kcal mol}^{-1}/(RT)) \text{ s}^{-1}$ and $k_{1atm} = 3.6 \times 10^{12} \exp(-7.05 \text{ kcal mol}^{-1}/(RT)) \text{ s}^{-1}$. Thus, dissociation is also found to be the dominant fate of the thermalized oxy radicals.

Introduction

Unsaturated hydrocarbon species are important reactive trace gases in the troposphere, originating from a number of natural and anthropogenic sources. The lighter alkenes, ethene and propene, are predominantly emitted from fossil fuel combustion, biomass burning, and the oceans.[1] The atmospheric oxidation of ethene and propene is initiated primarily by their reaction with OH and to a lesser extent via their reaction with ozone.[2] The OH-initiated oxidation of alkenes (general formula, $R_2C{=}CR_2$) mainly proceeds in the atmosphere via the production of a β-hydroxyalkoxy radical, $HOCR_2-CR_2O^\bullet$:

$$OH + R_2C{=}CR_2 \rightarrow HOCR_2-CR_2^\bullet \quad (1)$$

$$HOCR_2-CR_2^\bullet + O_2 \rightarrow HOCR_2-CR_2O_2^\bullet \quad (2)$$

$$HOCR_2-CR_2O_2^\bullet + NO \rightarrow HOCR_2-CR_2O^\bullet + NO_2 \quad (3)$$

Recent studies conducted in our laboratories[3,4] on the oxidation of ethene show that the β-hydroxyalkoxy radical formed in its oxidation ($HOCH_2-CH_2O^\bullet$) is subject to a chemical activation effect. That is, a large fraction of the energy available from the exothermic reaction of $HOCH_2-CH_2O_2^\bullet$ with NO is imparted to the $HOCH_2-CH_2O^\bullet$ radical such that about 25% of the radicals are borne above the 10−11 kcal/mol barrier for their decomposition via C−C bond rupture and thus decompose promptly (on a subnanosecond time scale). The remainder of the radicals are thermalized and react via decomposition or reaction with O_2 on a much slower (microsecond) time scale. Similar chemical activation effects have also been observed in the chemistry of halogenated alkoxy radicals.[5−7]

The OH-initiated oxidation of propene will proceed via the formation of two β-hydroxyperoxy radicals, with initial OH attack at the 1-position (reaction 4a) likely to dominate:[8]

$$OH + CH_2{=}CH-CH_3 \,(+O_2) \rightarrow HOCH_2-CH(OO^\bullet)-CH_3 \quad (4a)$$

$$\rightarrow CH_2(OO^\bullet)-CH(OH)-CH_3 \quad (4b)$$

Subsequent reaction of these peroxy radicals with NO, proceed-

† E-mail: Jozef.Peeters@chem.kuleuven.ac.be.
‡ E-mail: Orlando@acd.ucar.edu.

10.1021/jp990046i CCC: $18.00
Published on Web 05/29/1999

ing via peroxynitrite intermediates, will lead to the formation of internally excited β-hydroxyalkoxy radicals:

$$HOCH_2-CH(OO^\bullet)-CH_3 + NO \rightarrow [HOCH_2-CH(O^\bullet)-CH_3]^* + NO_2 \quad (5)$$

$$CH_2(OO^\bullet)-CH(OH)-CH_3 + NO \rightarrow [CH_2(O^\bullet)-CH(OH)-CH_3]^* + NO_2 \quad (6)$$

Each of these radicals can undergo facile C−C bond cleavage to an α-hydroxyalkyl radical and an aldehyde. Since the barrier is expected to be lower than for $HOCH_2CH_2O$,[9] prompt decomposition is likely to be important (reactions 7 and 8):

$$[HOCH_2-CH(O^\bullet)-CH_3]^* \rightarrow {}^\bullet CH_2OH + CH_3CHO \quad (7)$$

$$[CH_2(O^\bullet)-CH(OH)-CH_3]^* \rightarrow CH_2O + CH_3C^\bullet H(OH) \quad (8)$$

$$^\bullet CH_2OH + O_2 \rightarrow CH_2O + HO_2^\bullet \quad (9)$$

$$CH_3C^\bullet HOH + O_2 \rightarrow CH_3CHO + HO_2^\bullet \quad (10)$$

In addition, a portion of these β-hydroxyalkoxy species may be thermalized such that thermal decomposition and reaction with O_2 may occur in competition:

$$HOCH_2-CH(O^\bullet)-CH_3 \rightarrow {}^\bullet CH_2OH + CH_3CHO \quad (11)$$

$$^\bullet OCH_2-CH(OH)-CH_3 \rightarrow CH_2O + CH_3C^\bullet H(OH) \quad (12)$$

$$HOCH_2-CH(O^\bullet)-CH_3 + O_2 \rightarrow HOCH_2-C(O)-CH_3 + HO_2^\bullet \quad (13)$$

$$^\bullet OCH_2-CH(OH)-CH_3 + O_2 \rightarrow CH_3CH(OH)CHO + HO_2^\bullet \quad (14)$$

Previous experiments on the OH-initiated oxidation of propene[10] have been restricted to room temperature and 1 atm of air. In those experiments, formaldehyde and acetaldehyde were the only observed products, which implies that decomposition is the dominant if not the sole fate of the β-hydroxyalkoxy radicals near 298 K. However, it is not possible to discern from the previous experiments to what extent, if any, chemical activation is occurring. In addition, no studies have been carried out at lower temperature, where the possibility of the significant occurrence of reactions 13 and 14, and thus a change in the overall oxidation mechanism, is possible.

In this paper, a combined theoretical and experimental approach is used to study the oxidation of propene. In the experimental phase of the work, end products of the OH-initiated oxidation of propene are detected over a range of temperatures (220−298 K) in an attempt to elucidate the chemistry of the β-hydroxyalkoxy radicals produced in the oxidation of propene. In the theoretical phase of the work, a quantum chemical characterization is first performed of the dominant β-hydroxyalkoxy radical, $HOCH_2CH(O^\bullet)CH_3$, and of the transition state(s) to its decomposition in reactions 7 and 11, with due attention to the intramolecular hydrogen bond, the remarkable persistence of which during dissociation proved to be of crucial importance for the $HOCH_2CH_2O^\bullet$ radical.[3,4] Subsequently, separate statistical ensemble theory[3,4,11] is used to determine the energy distribution of the nascent β-hydroxyalkoxy radicals formed in reaction 5, and the fraction of radicals that decompose promptly before collisional deactivation can occur is then determined from a master equation analysis. Also, the rate of thermal decomposition is predicted using transition-state theory with corrections for falloff.

Experimental Section

Experiments were conducted in a 47 L stainless steel environmental chamber, which has been described elsewhere.[12,13] The temperature of the chamber is regulated from the flow of chilled ethanol from a circulating bath through a jacket surrounding the chamber. The chamber is interfaced to a Bomem DA3.01 Fourier transform infrared spectrometer via a set of Hanst-type multipass optics, which provide an infrared path length of 32.6 m. Infrared spectra were obtained at a resolution of 1 cm^{-1} from the co-addition of 50−250 interferograms.

Experiments were conducted over the range 220−298 K from the photolysis of mixtures of $^{13}CH_3ONO$ ($(1.4-7.0) \times 10^{15}$ molecule cm^{-3}), propene ($(0.5-1.1) \times 10^{15}$ molecule cm^{-3}), NO ($(0.2-1.5) \times 10^{15}$ molecule cm^{-3}), O_2 (150−1000 Torr), and N_2 (0−550 Torr) at total pressures of either 700 or 1000 Torr. Minor components of the mixture (propene, $^{13}CH_3ONO$, and NO) were swept with N_2 into the chamber from smaller calibrated volumes. Photolyses were carried out with a Xe arc lamp, filtered to provide radiation in the range 240−400 nm. The near-UV photolysis of CH_3ONO results in the production of OH:

$$^{13}CH_3ONO + h\nu \rightarrow {}^{13}CH_3O + NO \quad (15)$$

$$^{13}CH_3O + O_2 \rightarrow {}^{13}CH_2O + HO_2 \quad (16)$$

$$HO_2 + NO \rightarrow OH + NO_2 \quad (17)$$

which initiates the oxidation of propene via reaction 4. Use of isotopically labeled CH_3ONO allows for spectral differentiation between the CH_2O generated from the photolysis of CH_3ONO from that produced in the propene oxidation. Quantification of starting materials and products via FT-IR was accomplished from comparison with standard spectra obtained in our laboratory. $^{13}CH_3ONO$ was prepared from the addition of sulfuric acid to a saturated solution of $NaNO_2$ in $^{13}CH_3OH$, as described by Taylor et al.,[14] and purified by numerous freeze−pump−thaw cycles prior to use. Other gases were used as purchased: N_2 from the boil-off of a liquid N_2 Dewar, O_2 (UHP, U.S. Welding), C_3H_6 (C.P. Grade, Matheson), and NO (Linde).

Experimental Results

The OH-initiated oxidation of propene was studied first at room temperature over a range of O_2 partial pressures (150−1000 Torr). Under all conditions studied, formaldehyde and acetaldehyde were the only carbon-containing products observed in the oxidation. Furthermore, as shown in Figure 1, the yields of both CH_2O and CH_3CHO were found to be equal to unity, within experimental uncertainty (both 1.05 ± 0.10). That no hydroxyacetone was observed under any experimental conditions (even in the presence of 1000 Torr of O_2) is strong evidence for the dominance of the decomposition of the alkoxy radicals (reactions 7−12) over their reaction with O_2. These results are in agreement with those of Niki et al.,[10] who also observed unity yields of CH_2O and CH_3CHO in the OH-initiated oxidation of propene at 298 K and 1 atm of air.

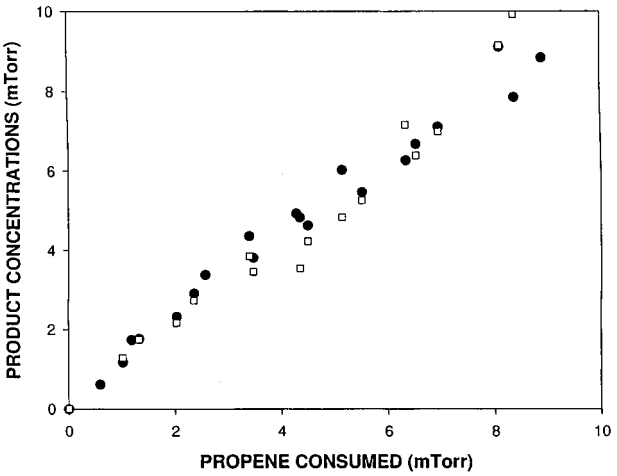

Figure 1. Observed concentrations of CH_2O (filled circles) and CH_3CHO (open squares) as a function of propene consumption in the OH-initiated oxidation of propene at 298 K, 700 Torr total pressure.

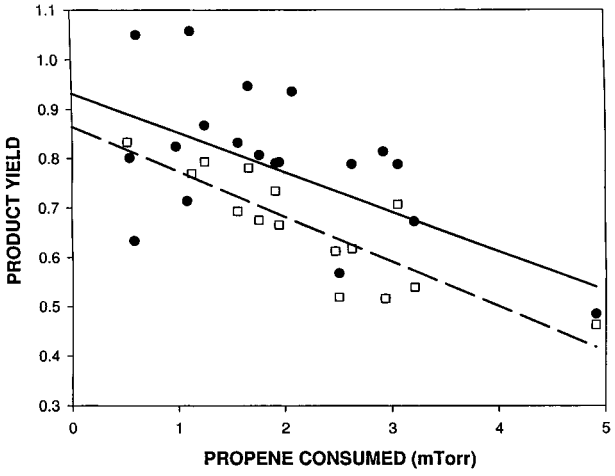

Figure 2. Molar yields of CH_2O (filled circles, solid line) and CH_3CHO (open squares, dashed line) from the OH-initiated oxidation of propene at 248 K, 700 Torr total pressure.

The results of lower temperature experiments were qualitatively similar to those obtained at room temperature. Again, under all conditions studied ($[O_2] = 100-1000$ Torr, $T = 220$, 233, and 248 K), the dominant carbon-containing products identified in the product spectra were CH_2O and CH_3CHO. However, the yields of these species were not uniform over the course of an experiment, decreasing with the extent of propene conversion. For example, at 248 K, as seen from Figure 2, the yields of both CH_3CHO and CH_2O decrease from approximately 0.9 at low conversions to approximately 0.5 at higher conversions. Though not as extensively studied, similar effects were seen at lower temperatures for both CH_2O and CH_3CHO. The reason for the decrease in CH_2O and CH_3CHO yields with propene conversion is likely related to the formation of peroxynitrate compounds. At early reaction times, the $[NO_2]/[NO]$ ratio is near zero, and the chemistry of the peroxy radicals generated in reaction 4 is dominated by their reaction with NO (reactions 5 and 6). However, as the extent of reaction increases and the $[NO_2]/[NO]$ ratio increases, reactions 18 and 19 become more important:

$$HOCH_2-CH(OO^{\bullet})-CH_3 + NO_2 + M \rightarrow HOCH_2-CH(O_2NO_2)-CH_3 + M \quad (18)$$

$$CH_2(OO^{\bullet})-CH(OH)-CH_3 + NO_2 + M \rightarrow CH_2(O_2NO_2)-CH(OH)-CH_3 + M \quad (19)$$

While these reactions are also occurring in the 298 K experiments, their effect is minimal because of the rapid thermal decomposition of the peroxynitrates (the reverse of reactions 18 and 19). At 298 K and 1 atm pressure, typical lifetimes for alkylperoxynitrates are less than 1 s; thus, formation of these species is reversible on the time scale of our chamber experiments, and the peroxy radicals are eventually converted to oxy radicals via reactions 5 and 6. However, at 248 K and below, the lifetime of the peroxynitrates increases to 10 mins or more and their formation becomes a permanent sink for the peroxy radicals, arresting the chemistry before formation of the oxy radical can occur.

Peroxynitrate species possess characteristic absorption features near 1300 and 1720 cm^{-1} (the NO_2 symmetric and asymmetric stretches, respectively).[15] The identification and quantification of the peroxynitrate species in the product spectra is complicated by the presence of such species as $^{13}CH_3ONO$, $^{13}CH_3ONO_2$, $^{13}CH_2O$ (products of $^{13}CH_3ONO$ photolysis), and possibly other nitrate species. However, some evidence for the existence of the peroxynitrates in the system was found by allowing irradiated samples to stand in the dark in the chamber for 30 min at 248 K. A decrease in absorption near 1300 and 1720 cm^{-1} was noted, consistent with loss of the peroxynitrate species via the reverse of reactions 18 and 19 and subsequent reaction of the peroxy radicals with NO. Assuming similar absorption cross sections for these species as is typical for alkylperoxynitrates, the amount of peroxynitrate species loss was about 10% of the initial amount of propene consumed in an experiment where the CH_2O and CH_3CHO yields were both 80−85%.

This tentative observation of peroxynitrate species in the low-temperature product spectra, coupled with yields of CH_2O and CH_3CHO near unity when extrapolated to low propene conversion, argues against significantly different behavior of the β-hydroxyalkoxy radicals at low temperature compared to their behavior near 298 K. Under no condition of temperature (220−248 K) or O_2 (100−600 Torr) was any hydroxyacetone observed in the product spectra, and an upper limit to its yield relative to that of CH_2O (and CH_3CHO) of 0.15 is obtained. That is, even under the conditions that most favor the formation of hydroxyacetone (220 K, 600 Torr of O_2), decomposition of the predominant β-hydroxyalkoxy radical, $HOCH_2CH(O^{\bullet})CH_3$, via reaction 7 and/or reaction 11 dominates over its reaction with O_2 by a factor of 6 or 7.

The experiments discussed above are sufficient to determine the atmospheric fate of propene in the atmosphere; it is clear that decomposition of the β-hydroxyalkoxy radicals will dominate under the temperature and O_2 partial pressures encountered throughout the troposphere. However, it is still unclear on the basis of these data to what extent the decomposition of the β-hydroxyalkoxy radicals occurs via chemical activation. The lack of hydroxyacetone formation does imply either (a) that a large fraction of the alkoxy radicals are chemically activated and decompose prior to undergoing collisions, pre-empting the possibility of thermalization and subsequent reaction with O_2, or (b) that a significant yield of thermalized radicals is obtained but that the barrier to their decomposition is sufficiently low such that reaction with O_2 cannot compete with their decomposition, even at 220 K and 600 Torr of O_2. The extent of chemical activation of the β-hydroxyalkoxy radicals obtained in the OH-initiated oxidation of propene and the importance of

TABLE 1: Zero-Point-Energy-Corrected Relative Energies for All Rotamers of β-Hydroxypropoxy Radicals, the Transition States for C−C Bond Rupture, and the Reaction Products

structure[a]	dihedral angle (deg) OCCO	dihedral angle (deg) HOCC	chiral orientation	energy ($\langle S^2 \rangle$[b]) hartree	ZPE kcal/mol	rel energy kcal/mol
β-Hydroxypropoxy Radicals, $HOCH_2CH(O^{\bullet})CH_3$						
mpR	−48.1	43.2	R	−268.906 290 1 (0.7533)	60.17	0.00
pmR	51.9	−46.7	R	−268.905 273 5 (0.7531)	60.64	1.11
ttR	−170.3	−175.6	R	−268.900 902 3 (0.7531)	59.72	2.93
tpR	−178.8	72.5	R	−268.901 561 8 (0.7531)	60.18	2.98
tmR	−177.7	−78.9	R	−268.900 690 5 (0.7531)	60.10	3.44
ppR	72.2	70.8	R	−268.899 870 9 (0.7535)	60.09	3.95
mmR	−66.0	−63.5	R	−268.899 721 8 (0.7535)	60.17	4.12
ptR	74.4	176.5	R	−268.898 579 7 (0.7530)	59.65	4.32
mtR	−66.9	161.6	R	−268.898 743 0 (0.7530)	59.87	4.43
Transition States for C−C Bond Rupture in $HOCH_2\cdots CH(O^{\bullet})CH_3$ and Dissociation Products						
TS_mpR	−47.8	43.6	R	−268.892 285 4 (0.7607)	58.62	7.24
TS_pmR	51.3	−49.6	R	−268.890 764 0 (0.7611)	58.76	8.33
TS_tpR	−176.8	80.5	R	−268.888 216 0 (0.7637)	58.48	9.65
TS_tmR	174.1	−82.4	R	−268.887 982 8 (0.7638)	58.54	9.85
TS_ppR	81.9	78.3	R	−268.885 189 8 (0.7645)	58.46	11.53
TS_mmR	−53.6	−75.0	R	−268.884 746 0 (0.7637)	58.29	11.64
$CH_3CHO\cdots HOC^{\bullet}H_2$ (H-bonded complex)				−268.906 262 4 (0.7530)	57.82	−2.33
$CH_3CHO + {}^{\bullet}CH_2OH$ (infinite separation)				−268.891 468 5 (0.7529)	56.18	2.15[c]

[a] The name is based on the dihedral angles and the chiral orientation: "p" for a dihedral angles of about +60°, "m" for about −60°, and "t" for angles close to 180°. [b] Spin operator expectation value of the DFT wave function before annihilation of the first contaminant; for the separated product, the value for $^{\bullet}CH_2OH$ fragment is reported. [c] Corrected for BSSE.

their ensuing prompt decomposition will be determined from the theoretical analysis discussed below.

Computational Methods

The geometry optimizations and subsequent frequency calculations were performed at the B3LYP-DFT level of theory, i.e., Becke's three-parameter nonlocal-exchange functional[16] with the nonlocal correlation functional of Lee, Yang, and Parr.[17] The basis set used was 6-31G** for all calculations. The vibrational frequencies reported here have been systematically scaled by a factor of 0.9614, as reported by Scott and Radom[18] for the 6-31G* basis set. We provided an extensive validation of B3LYP-DFT/6-31G** for hydroxyalkoxy radicals in an earlier study.[4] Briefly, B3LYP-DFT/6-31G** values for the crucial energy barrier to C−C bond rupture in alkoxy radicals are within about 0.5−1.0 kcal/mol of available experimental data for such processes, which range from 10 to 20 kcal/mol. Moreover, DFT is known to be an adequate computational tool for hydrogen bonds.[19,20] Since dissociation barrier heights and hydrogen bond stabilization energies are the key energetic quantities to this study of β-hydroxypropoxy radicals, we chose not to perform costly higher-level calculations but to rely here entirely on B3LYP-DFT/6-31G** results. No significant spin contamination was found for the DFT wave functions of the β-hydroxyalkoxy radicals and of the transition states in their decomposition (see Table 1); after annihilation of the first spin contaminant, $\langle S^2 \rangle$ becomes 0.7500 in all cases. The relative energy for the β-hydroxypropoxy dissociation products needs to be corrected for basis set superposition errors (BSSE). As argued by Van Duijneveldt et al.,[21] this can be correctly estimated using the Boys−Bernardi counterpoise procedure,[22] in which the energy of each fragment is calculated at the geometry it has in the parent molecule, both with and without the presence of the ghost orbitals of the other fragment. The BSSE correction lowers the relative energy of the products at infinite separation by 3.2 kcal/mol. The Gaussian 94 program suite[23] was used for all quantum chemical computations.

Quantum Chemical Characterization

The β-hydroxypropylperoxy radicals, β-hydroxypropylperoxynitrite molecules, and β-hydroxypropoxy radicals, all intermediates in the OH-initiated oxidation of propene as outlined above, have several degrees of freedom for internal rotation and therefore exhibit extensive internal rotational isomerism. Furthermore, some of the rotamers of the β-hydroxyalkylperoxy and -alkoxy radicals[3,4] and some of their peroxynitrites[24] can be stabilized by intramolecular hydrogen bonding between the hydroxy H and an oxygen of the (per)oxy function. Our earlier study of the β-hydroxyeth(ylper)oxy radicals[4] revealed that the relative energies of the different rotamers for the hydroxyalkylperoxy radicals are comparable to those of the hydroxyalkoxy radical rotamers. Their exact relative energies do not influence the reaction kinetics for the oxidation of the alkene profoundly and were therefore not considered explicitly in the present work.

According to a recently developed site-specific structure−activity relationship for alkene + OH reactions,[8] the branching ratio k_{4a}/k_{4b} of the initial propene + OH reaction is expected to be 85:15; product distributions that could be measured directly for a few alkenes agree with the SAR predictions within 5−10% (absolute).[25] The above is consistent with our finding that the secondary 1-hydroxy-2-propyl radical, formed in reaction 4a, is 1.7 kcal/mol more stable than the primary 2-hydroxy-1-propyl radical, formed in reaction 4b. We therefore limit the full theoretical analysis to the dominant oxidation route initiated by reaction 4a. The geometry of the radical center of $HOCH_2C^{\bullet}HCH_3$ is near-planar, with the unpaired electron of the central carbon in a p-orbital perpendicular to the plane. Subsequent combination with O_2, in reaction 4a, can occur at both sides of the plane with equal probabilities, resulting in 1-hydroxy-2-propylperoxy radicals $HOCH_2CH(OO^{\bullet})CH_3$ with a chiral central carbon, and hence in equal amounts of R- and S-forms of both the peroxy radical and the oxy radical $HOCH_2CH(O^{\bullet})CH_3$ generated by reaction 5.

The 1-hydroxy-2-propoxy radicals, referred to as "the oxy radicals" from here on, have three degrees of freedom for internal rotation. The dihedral angles O−C−C−O and H−O−

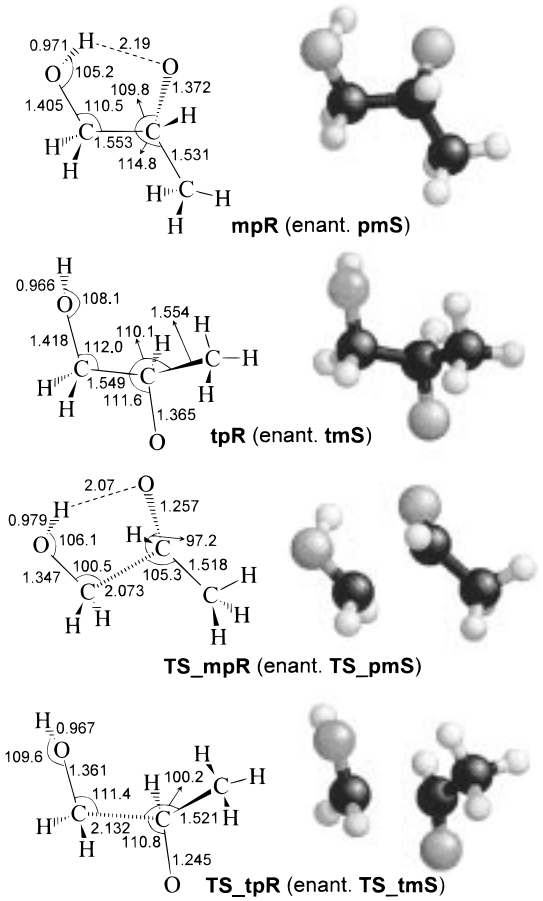

Figure 3. Selected geometric parameters for rotamers of the $HOCH_2$-$CH(O^{\bullet})CH_3$ radicals and the transition states for C−C bond rupture in these radicals. Bond lengths are in angstroms and angles in degrees.

C−C each have three values corresponding to a minimum in energy; the third internal rotation corresponds to the rotation of the CH_3 group and is degenerate. Also, because of the chiral central carbon, we have both an R- and S-form. The 18 ($=3 \times 3 \times 2$) distinct $HOCH_2CH(O^{\bullet})CH_3$ internal-rotation conformers can be paired (by inverting the sign of all dihedral angles) in 9 pairs of enantiomers with the same energy. The transition states for dissociation of the oxy radical to $^{\bullet}CH_2OH$ and CH_3CHO have near-planar CH_2OH moieties, where the stereochemical interaction is such that only two values for the H−O−C−C dihedral angles correspond to a local minimum in energy, leading to 12 ($=3 \times 2 \times 2$) $HOCH_2\cdots CH(O^{\bullet})CH_3$ transition-state conformers, i.e., six pairs of enantiomers. We will limit the following discussion to the R-conformers; their enantiomers behave identically.

Table 1 lists the ZPE-corrected relative energies for all rotamers of the 1-hydroxy-2-propoxy radicals, $HOCH_2CH(O^{\bullet})$-CH_3, as well as for all rotamers of the transition state for C−C bond rupture in these radicals, $HOCH_2\cdots CH(O^{\bullet})CH_3$. The only coordinates given in Table 1 are the dihedral angles O−C−C−O and H−O−C−C and the chiral orientation of the center carbon, since they define the different rotamers. The complete geometrical specifications can be found in the Supporting Information. Figure 3 shows some of the rotamers; a three-dimensional representation of the complete set of structures is included in the Supporting Information. Also included there is a listing of the vibrational wavenumbers for all molecules characterized in this study.

The relative energies of the different internal-rotation conformers are determined by steric hindrance, by Coulombic attraction and repulsion between the partially charged atoms, and, where geometrically possible, by hydrogen bonding. Two of the nine energetically different oxy rotamers (**mpR** and **pmR**) are stabilized by intramolecular hydrogen bonding, with a H···O distance of 2.19 and 2.25 Å, respectively. The other non-H-bonded oxy radicals have H···O distances above 3.4 Å with relative energies at least 1.8 kcal/mol above the least stable H-bonded structure, clearly showing the stabilizing effect of the intramolecular hydrogen bond. According to the DFT energy, geometry, and vibrational data, a thermal population of 1-hydroxy-2-propoxy radicals at 298 K should consist of 98% H-bonded rotamers.

A comparable stabilization by intramolecular H-bonding is found for the C−C cleavage transition states, $HOCH_2\cdots CH(O^{\bullet})$-$CH_3$; the two lowest decomposition transition states **TS_mpR** and **TS_pmR** have H···O distances of 2.07 and 2.21 Å, respectively, with relative energies of 7.2 and 8.3 kcal/mol above the most stable oxy radical **mpR**. The other transition states are not stabilized by intramolecular hydrogen bonding (H···O distance of >3.4 Å) and have relative energies of ≥ 9.5 kcal/mol above the energy of **mpR**. The persistence of the H-bonding during the C−C cleavage in **mpR** is possible only because both the CH_2OH and $CH(O)CH_3$ moieties become planar simultaneously with the elongation of the C−C bond in such a way that, up to and somewhat beyond the transition state, only the two separating C atoms move significantly. As a result of the H-bond persistence, the energy difference between the lowest TS (**TS_mpR**) and its H-bonded oxy radical parent (**mpR**) is only slightly higher than the difference between the (lowest) non-H-bonded TS (**TS_tpR**) and its non-H-bonded oxy radical parent (**tpR**); both differences are within 0.3 kcal/mol of 7 kcal/mol. As extensively argued for the ethene case,[4] the persistence of the H-bond in transition states is a crucial factor in the dissociation of β-hydroxyalkoxy radicals. Other observations confirm the intramolecular hydrogen bonding in the lowest-lying oxy radicals and transition states. Characteristic for hydrogen bonds is the downward frequency shift for the OH stretch vibration. This shift can be clearly seen for both the **mpR** and **pmR** minima ($\Delta\nu \approx -60$ cm^{-1}) and the corresponding transition states ($\Delta\nu \approx -180$ cm^{-1}). The hydrogen bond also enhances the rigidity of the structure, which increases the wavenumbers for some of the lowest vibrations.

Attack of the OH radical on the 2-position in propene (reaction 4b), giving 2-hydroxy-1-propyl radicals, constitutes the minor reaction path.[8] Sample calculations indicate that the relative energies and vibrational characteristics of the resulting oxy radicals and decomposition transition states are comparable to those for the main channel. Thus, the most stable 2-hydroxy-1-propoxy rotamer has a relative energy only 0.4 kcal/mol below the energy of the 1-hydroxy-2-propoxy **mpR** rotamer, and the lowest dissociation barrier for the 2-hydroxy-1-propoxy radicals (reactions 8 and 12) is 7.0 kcal/mol. Therefore, taking the minor channel into account explicitly should have only a minor effect on the theoretical kinetic predictions described below.

For all reaction conditions considered, rapid interconversion of the different oxy rotamers is possible through transition states approximately 0.5−1.5 kcal/mol above the highest of the two pertaining minima. These transition states were not characterized directly; they should be comparable to the results for the β-hydroxyethoxy rotamerization.[4] In view of the heights of the energy barriers for dissociation compared to those for internal rotation, rotamerization will occur much more rapidly than dissociation, ensuring fast (microcanonical) equilibration under atmospheric conditions.

Other intramolecular rearrangements are possible in the molecules considered, in particular a hydrogen shift from the OH group to the radical oxygen, aided by the H-bond. As discussed in our previous paper,[4] a 1,5-hydrogen transfer in β-hydroxyethylperoxy radicals was not found to be important because of the high endothermicity of ~19 kcal/mol of this reaction and the lack of subsequent reactions preventing the simple reisomerization to the original ethylperoxy radicals. Substituting a H atom for a CH_3 group, forming the homologous β-hydroxypropylperoxy radicals, hardly affects the chemical sites relevant for the H migration considered. The endothermicity for a 1,5-hydrogen transfer in those latter radicals should therefore be comparable to that for the hydroxyethylperoxy case such that this isomerization can be neglected. In β-hydroxypropoxy radicals, on the other hand, 1,4-hydrogen migrations could conceivably occur. Yet thermal isomerization of oxy radicals by a 1,4-hydrogen shift is known to be negligibly slow compared to reaction with O_2.[9] For the $HOCH_2CH(O^\bullet)CH_3 \leftrightarrow {}^\bullet OCH_2CH(OH)CH_3$ reaction, which amounts to an interconversion of the two types of oxy radicals possible in the oxidation of propene, the DFT barrier height is calculated at 12.1 kcal/mol (see Supporting Information) such that this process will be outrun by C−C bond cleavage, which faces a barrier of only about 7 kcal/mol.

Kinetics of "Prompt" and Thermal Decomposition of β-Hydroxypropoxy Radicals: Theoretical Quantification

In a first subsection, a quantum statistics based master equation analysis is described, aiming to quantify the fraction of 1-hydroxy-2-propoxy radicals formed in reaction 5 that dissociate "promptly", i.e., before collisional thermalization. The methodology of these calculations, as implemented in our URESAM computer program suite,[26] has been already described in earlier work,[4] where we applied it to the corresponding process in the oxidation of ethene, resulting in theoretical predictions[3,4] in excellent agreement with the experimental results.[3] Here, only the basic outlines of the methodology will be given, emphasizing the elements where the propene case differs from the ethene case.

Four steps can be discerned: (i) reaction of the $HOCH_2CH(OO^\bullet)CH_3$ radical with NO to form a vibrationally excited $HOCH_2CH(CH_3)OONO^*$ peroxynitrite, of which the thermal internal-energy distribution at formation is obtained from the sum of states $G^\ddagger(E-E_0)$ of the (variational) entrance transition state;[27] (ii) during its lifetime, the chemically activated peroxynitrite may suffer collisional energy loss and hence a change in its internal energy distribution, which is quantified by RRKM-based master equation analysis; (iii) dissociation of the activated peroxynitrite into NO_2 and the $HOCH_2CH(O^\bullet)CH_3$ oxy radical, with partitioning of the available energy over the products calculated by an appropriate statistical theory (provided that ergodicity applies, i.e., that the peroxynitrite lifetime is $\geq 10^{-12}$ s^{-1}); (iv) prompt dissociation of a fraction of the resulting activated oxy radicals in competition with their collisional thermalization, quantified by a second RRKM-based master equation analysis.

(i) A major share of the energy available to the dissociation products of the peroxynitrite is provided by the overall exoergicity of reaction 5. Since the H-bond stabilization is nearly equal for β-hydroxyalkylperoxy and β-hydroxyalkoxy radicals,[4] the exoergicity can be taken to be equal to that of the analogous reaction of unsubstituted isopropylperoxy radicals, i.e., 10 kcal mol^{-1}.[28]

(ii) To estimate the lifetime of the peroxynitrite and to perform the master equation analysis for this step, one also needs the relative energy of the peroxynitrite equilibrium structures; we adopted values 14 kcal mol^{-1} below the level of the corresponding oxy rotamer + NO_2,[24] consistent with the analogous 2-butyl case.[29] Evaluation of the distribution[27] of the thermal internal energy E_{th} of the entrance transition state leading to peroxynitrite, $F_{form}(E)$, needed for both steps i and ii requires estimates of the vibrational frequencies of the variational entrance TS. The average E_{th} at 300 K is about 5 kcal/mol; E_{th} will contribute to the internal energy imparted to the peroxynitrite dissociation products. The peroxynitrite* dissociation rate constants were obtained using RRKM theory;[27] densities of states of the peroxynitrite and sums of states for the entrance and exit channels were obtained by exact count.[30] Since the lifetime is not critical in this case and the calculated energy distribution is not very sensitive to the exact vibrational frequencies, we used estimated vibrational frequencies for the peroxynitrite and for the entrance and exit transition states without resorting to a rigorous variational treatment. Thus, the average RRKM lifetime for dissociation of the activated peroxynitrite* is found to be approximately 2×10^{-10} s. Given the collision frequency for 1 atm of air at 300 K of 1.1×10^{10} s^{-1} (using the estimated collision parameters $\epsilon_{A-A} = 313$ K and $\sigma_A = 6$ Å), it follows that the peroxynitrite does indeed lose a small fraction of its internal energy by collisions such that a master equation analysis is required. For the ethene case, the peroxynitrite dissociates much faster, without suffering collisional energy loss.[3,4] Collisional energy transfer is incorporated in the master equation using Troe's biexponential model,[31] with an estimated average energy transfer $\langle \Delta E_{tot} \rangle$ of -150 cm^{-1}.[32] Partially stabilized peroxynitrite molecules, with an internal energy less than 7 kcal/mol, are collected in a sink; the results are not sensitive to the exact cutoff value used. About 4% of the peroxynitrite molecules formed are thermalized at room temperature and 1 atm total pressure, increasing to 20% at 200 K. The internal energy distribution of the peroxynitrite molecules on dissociation, $F_{diss}(E)$, is shifted downward compared to the nascent energy distribution $F_{form}(E)$. At 300 K and 1 atm, the average energy loss is ~2 kcal/mol. As shown in Table 1, the energy loss in the peroxynitrite molecules has only a limited effect on the calculated prompt dissociation fraction of the 1-hydroxy-2-propoxy radicals. The change in internal energy of the peroxynitrite dissociation TS with respect to the entrance TS, imposed by the conservation of angular momentum and by the small changes in the moments of inertia, should be at most $\sim kT$ and was therefore neglected here as in the analogous $HOCH_2CH_2OONO$ case.[4] At 300 K and 1 atm, the average internal energy $\langle E_{tot} \rangle$ available to the peroxynitrite dissociation products $HOCH_2CH(O^\bullet)CH_3 + NO_2$, taking into account the collisional loss of ~2 kcal/mol, is therefore ~13 kcal/mol.

Formation of the hydroxypropylnitrate in reactions 5 and 6 is limited to only 1.5%, as recently reported by O'Brien et al.,[24] and can therefore be neglected in the present study. Yet it is worth mentioning here that the general mechanism of nitrate formation in RO_2 + NO reactions is not well understood. Concerted isomerization of ROONO* to $RONO_2$ appears to be unlikely on the grounds that the calculated barrier to concerted isomerization for the model reaction $HOONO \rightarrow HONO_2$ is as high as 60 kcal/mol.[33] We could not locate a $ROONO \rightarrow RONO_2$ isomerization saddle point for $R = HOCH_2CH_2$; an earlier attempt for R = 2-butyl also failed.[29] The suggestion by O'Brien et al.[24] that nitrates arise by recombination of the (nearly) separated RO + NO_2 dissociation products of ROONO awaits confirmation.

(iii) The 1-hydroxy-2-propylperoxynitrite molecules, containing an internal energy of some 15 kcal/mol in excess of the 14 kcal/mol barrier, have a fairly long (RRKM) lifetime of $\sim 2 \times 10^{-10}$ s. There is a great body of evidence that for molecules with at least four atoms containing more than ~20 kcal/mol of internal energy, the energy is in general randomly redistributed over all vibrational modes in about 10^{-12} s; hence, the lifetime of 2×10^{-10} s amply ensures ergodicity. Since internal rotamerization rate constants are $\geq 10^{11}$ s^{-1}, this lifetime also leads to a microcanonical equilibrium between all rotamers. This implies that the various oxy rotamers will be formed in relative contributions proportional to their respective densities of states and therefore in accordance with their relative energies. Furthermore, the dissociation of an alkylperoxynitrite to an oxy radical + NO_2 occurs through a barrierless exit channel[29] characterized by a late and loose transition state. Under these conditions, the nascent vibrational energy distributions for the resulting oxy radical rotamers can be obtained according to the extended separate statistical ensemble (SSE) theory of Wittig et al., which has been validated for a number of processes.[11] This theory and its extension as well as the conditions for its applicability have already been discussed in depth and applied in the study of the oxidation of ethene.[3,4] SSE theory evaluates a statistical distribution of the total available internal energy E_{tot} over the vibrational degrees of freedom of each of the two dissociation fragments and over the degrees of freedom for their relative motion by adopting equal probabilities for each discrete quantum state of the separating products. As discussed by Wittig et al.,[11] an important and explicit difference of the SSE from phase space theory is that SSE recognizes that there is no free flow of energy between the degrees of freedom of overall rotation and the internal degrees of freedom such that only the internal (=vibrational) energy of a parent molecule is freely available for distribution over the separating fragments. The SSE formula below describes the probability $P_{A_i}(E_A)$ of forming a hydroxyalkoxy fragment in rotameric form i with a certain energy E_A, given that a total energy E_{tot} is available for distribution over the oxy radical fragment, the NO_2 fragment, and the six degrees of freedom for their relative translation and rotation:

$$P^{E_{tot}}_{A_i}(E_A) = [N_{A_i}(E_A)\int_0^{E_{tot}-E_A}[N_{NO_2}(E_{NO_2})N_{rel.mot.}(E_{tot} - E_A - E_{NO_2})]\,dE_{NO_2}]/$$
$$[\int_0^{E_{tot}}\{(\sum_i N_{A_i}(E_A))\int_0^{E_{tot}-E_A}[N_{NO_2}(E_{NO_2})N_{rel.mot.}(E_{tot} - E_A - E_{NO_2})]\,dE_{NO_2}\}\,dE_A]$$

This probability depends on the energy dependence of the individual density of states $N(E)$; for the oxy and NO_2 fragments the $N(E)$ were obtained by exact count[30] using the DFT rovibrational data. The density of states for relative motion are treated as unhindered free particle motions with a combined state density varying therefore as $E^{(6/2)-1}$. To obtain the probability of formation of an oxy rotamer i with vibrational energy E_A, the equation above has to be integrated over the E_{tot} distribution, $F_{diss}(E)$, determined in step ii above; summing over all rotamers gives the probability $P_{form}(E_A)$ of formation of oxy radicals with internal energy E_A. Figure 4 shows the combined internal energy distribution $P_{form}(E_A)$ of the oxy radicals for initial reactants at 300 K; the contribution $P_{form}(E_{A_i})$ for each of the rotamers i is proportional to their density of states at the considered energy relative to the ground-state energy of the most stable rotamer.

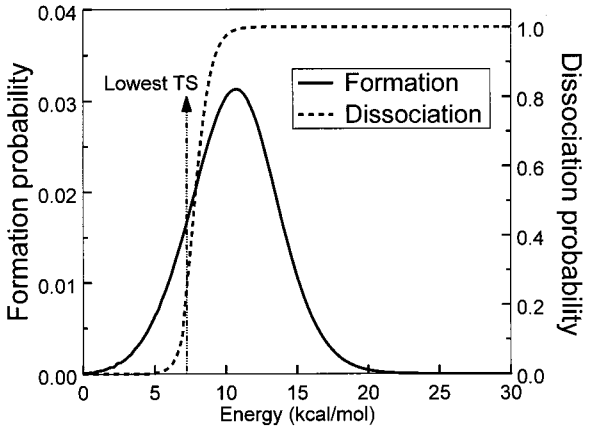

Figure 4. Predicted nascent vibrational energy distribution $P_{form}(E_A)$ for the $HOCH_2CH(O)CH_3$ oxy radicals formed in reaction 5 at 300 K; energy grain size = 0.239 kcal/mol. Predicted probability $f(E_A)$ of prompt dissociation at 1 atm.

(iv) The $HOCH_2CH(O^\bullet)CH_3$* radicals formed in reaction 5 will then either decompose promptly or assume a thermal energy distribution by collisional energy transfer with bath gas molecules. The relative importance of these two processes is quantified by master equation analysis, in a way similar to that described above. $P_{form}(E_{A_i})$ is used as the nascent energy distribution for the oxy radicals. Energy-specific dissociation rates for the various oxy radicals were obtained by RRKM theory, using the B3LYP-DFT/6-31G** energy barrier and vibrational frequency data of the previous section. The average energy transferred per collision with the bath gas was estimated at $\langle \Delta E_{tot} \rangle = -130$ cm^{-1}.[32] Rotamerization was incorporated by allowing internal rotation, but of only one internal rotor at a time. A barrier height of 5 kcal/mol was used for these reactions, which is an estimated upper limit; the sum of states was calculated on the basis of frequencies obtained in sample DFT calculations for isomerization transition states. Isomerization is sufficiently fast to maintain microcanonical equilibrium between the different rotamers during dissociation and collisional thermalization; even the rate constants for the slowest isomerizations starting from the two most stable rotamers, averaged over the activated population, are about 5×10^{10} s^{-1}, an order of magnitude faster than the rate constants for prompt dissociation, $k_{diss} \leq 4 \times 10^9$ s^{-1}. Under thermal conditions, the ratio of isomerization to dissociation should be higher still. Obviously, isomerization by inversion of the chiral center has too high an energy barrier to be significant, but since every R rotamer has a chemically identical S-enantiomer, the results for both sets of rotamers should be identical. Molecules with an internal energy below the isomerization transition states are assumed to be stabilized and are collected in a sink. Thermal reactivation occurs on a much slower time scale ($k_{therm} < 2.5 \times 10^7$ s^{-1}; see below) than prompt dissociation ($k_{diss} \geq 10^9$ s^{-1}), supporting the use of a sink to separate "prompt" from "thermal" dissociation; the results obtained are not sensitive to the exact cutoff energy adopted. The large difference in time scale for the prompt versus thermal dissociation also indicates that the description would not benefit from the use of a single, time-dependent rate constant for dissociation for the entire analysis, since this rate constant will very quickly converge to the thermal dissociation rate constant. Figure 4 shows the probability $f(E_A)$ of prompt dissociation of oxy radicals formed with a given internal energy E_A for reaction conditions of 300 K and 1 atm. The overall fraction of oxy radicals formed that dissociate promptly is finally obtained from the integral of the product $P_{form}(E_A)f(E_A)$. Thus, we predict a prompt dissociation fraction of 80% at 1 atm of

TABLE 2: Results of the Master Equation Calculations on Prompt Dissociation of β-Hydroxypropoxy Radicals Formed in the RO_2 + NO Reaction for Several Combinations of Reaction Parameters

parameter varied	value used[a]	prompt dissociation fraction (%)
height of H-bonded TSs, **TS_mpR/TS_pmR**, other TSs unchanged (kcal/mol)	**7.24/8.33**	79.7
	7.50/**8.33**	76.7
	8.00/**8.33**	70.8
	7.50/8.59	76.4
	8.00/9.09	68.6
	8.50/9.59	60.6
	9.00/10.09	53.1
	9.50/10.59	47.7
exoergicity of the RO_2 + NO reaction (kcal/mol)	**10**	79.7
	11	86.6
	0.25	87.6
	0.50	84.2
	0.75	81.8
total pressure of air (atm)	**1.00**	79.7
	1.25	78.0
	1.50	76.6
	1.75	75.3
	2.00	74.1
	5.00	65.5
temp (K)	**300**	79.7
	275	74.5
	250	68.3
	225	61.2
	200	53.3
temp and pressure	220 K, 0.2 atm[b]	74.4
energy loss in ROONO	neglected	84.0

[a] Numbers in bold are the default values for the parameter. [b] Reaction conditions at the top of the troposphere (altitude of 15 km).

air and 300 K; i.e., a large majority of the $HOCH_2CH(O^\bullet)CH_3$ formed in reaction 5 immediately dissociates to $^\bullet CH_2OH$ + CH_3CHO, while only 20% are collisionally thermalized and will subsequently decompose thermally or react with O_2. Table 2 summarizes the sensitivity of this result to a number of parameters. The prompt dissociation fraction under atmospheric conditions, with pressure and temperature both decreasing with altitude, is almost constant; for the reaction conditions found at the top of the troposphere we find a fraction of 74% dissociation, only slightly lower than at sea level. The expected error in the predicted prompt dissociation fractions is evaluated to be about 10−15% by assuming an error on the dissociation barrier heights of 0.5−1 kcal/mol; this is the average deviation between the calculated B3LYP-DFT/6-31G** values and the experimental activation energy data for ethoxy, isopropoxy, and β-hydroxyethoxy radicals, for which rate measurements are available.[4]

The rate of thermal dissociation for the stabilized $HOCH_2CH(O^\bullet)CH_3$ radicals, reaction 11, can be estimated using transition-state theory (TST) and Troe's low-pressure theory,[31,34] yielding the high- and low-pressure limits, respectively, from which the rate constant at a specific pressure is then derived using Troe's falloff formalism.[34] Alternatively, the pressure-dependent thermal rate constant could be derived from a RRKM master equation analysis. Thermal rate constants, however, are much more sensitive than activated rate constants to effects of overall rotation, anharmonicity, and internal rotations; parameters for the impact of these effects are readily incorporated in the Troe formalism, whereas the more rigorous RRKM description requires the input of anharmonicity constants, etc., which are harder to quantify. For a thermal equilibrium population at 298 K, only the most stable, H-bonded oxy radical rotamers will contribute significantly; the relative population **mpR**/**pmR**/**ttR**/**tpR** of the four lowest rotamers is 1.000:0.133:0.012:0.011. Likewise, the H-bond stabilized transition states will account for the bulk of the reaction flux, with higher-lying transition states accounting for only a few percent: **TS_mpR**/**TS_pmR**/**TS_tpR**/**TS_tmR** = 1.000:0.156:0.029:0.021. All other minima and transition states have negligible relative populations.

The TST expression for the thermal high-pressure rate constant for multiple minima, interconnected by fast equilibrated isomerization channels and dissociating through multiple transition states, is

$$k_\infty = \frac{kT}{h}\frac{Q^\ddagger}{Q} e^{-E_0/(RT)} = \frac{kT}{h}\frac{\sum Q^\ddagger_{vib,rot} Q^\ddagger_{el}}{\sum Q_{vib,rot} Q_{el}} e^{-E_0/(RT)} = A_\infty(T)\, e^{-E_0/(RT)}$$

On the basis of the rovibrational characteristics and relative energies obtained in the quantum chemical DFT study, we calculate at 298 K a partition function ratio $Q^\ddagger/Q = 1.75$. The impact of the higher-lying rotamers without internal H-bond on this ratio is only about 2%. Combining the resulting preexponential factor A_∞(298 K) = 1.09×10^{13} s^{-1} with the theoretical barrier height E_0 = 7.24 kcal/mol leads to a high-pressure rate coefficient $k_\infty = 5.3 \times 10^7$ s^{-1} at 298 K. The low-pressure limit is calculated using the Troe equation:[34]

$$k_0 = kTZ_{LJ}[M]\beta\frac{N(E_0)\, e^{-E_0/(kT)}}{Q_{vib}} F_E F_{anh} F_{rot} F_{int.rot}$$

with the Lennard-Jones collision frequency $Z_{LJ} = 4.1 \times 10^{-10}$ cm^3 $molecule^{-1}$ s^{-1} at 298 K and M = N_2, using estimated collision parameters for the oxy radicals of ϵ_{A-A} = 391 K and σ_A = 5.0 Å. The adopted $\langle \Delta E_{tot} \rangle$ of −130 cm^{-1} can be converted into a collision efficiency $\beta = 0.22$. Since this reaction is nearly in its high-pressure regime at 1 atm, the value of the low-pressure rate coefficient k_0 has only a small effect on the calculated thermal rate coefficient under atmospheric conditions. Furthermore, including higher-lying rotamers in the calculation of k_0 affects the value by only a few percent. Therefore, for reasons of simplicity, we only consider the most stable oxy radical rotamer and dissociation transition state explicitly in evaluating k_0. The vibrational density of states $N(E_0)$ for **mpR** is equal to 1.77×10^4 states per kcal/mol, by exact count,[30] and Q_{vib} = 9.93 at 298 K. By use of Troe's formulas,[34] the energy dependence of the density of states F_E is estimated to be 1.52 and the correction for anharmonicity to be F_{anh} = 1.11. The moments of inertia for the transition states are comparable to those of the minima ($I^\ddagger/I$ = 1.08), so the effect of overall rotation is fairly small: F_{rot} = 1.76. The 1-hydroxy-2-propoxy radicals have three degrees of freedom of internal rotation, with barriers in the H-bonded rotamers that are high compared to kT. Treating each rotor as an oscillator with an estimated individual anharmonicity factor of 1.75,[34] we find a correction factor for internal rotation $F_{int.rot}$ = 5.36. Thus, with [M] at 1 atm and 298 K equal to 2.46×10^{19} $molecules/cm^3$, the low-pressure first-order rate coefficient is evaluated to be $k_0 = 1.8 \times 10^8$ s^{-1}. On the basis of k_∞, k_0, and an estimated broadening factor F_{cent} of 0.5, we finally obtain a thermal dissociation rate coefficient $k_{1atm,298K}$ at a pressure of 1 atm and 298 K equal to 2.4×10^7 s^{-1}, about a factor 2 below the high-pressure limit. The thermal rate coefficient at a temperature of 220 K, the lowest temperature in the experiments, can be calculated similarly. The high-pressure rate coefficient is found to be $k_\infty = 4.6 \times 10^5$ s^{-1}. For the calculation of the low-pressure rate

coefficient, the following parameters are different from the 298 K values: $Z_{LJ}[M] = 1.18 \times 10^{10}$ cm^3 molecule^{-1} s^{-1}; $Q_{vib} = 4.06$; $\beta = 0.29$; $F_E = 1.35$; $F_{rot} = 2.4$; $F_{rot.int} = 8$ (=2^3).[34] This results in a low-pressure first-order rate coefficient of $k_0 = 1.2 \times 10^7$ s^{-1}. Using $F_{cent} = 0.5$, we obtain a thermal rate coefficient at 220 K and 1 atm of $k_{1atm,220K} = 3.5 \times 10^5$ s^{-1}, only a factor of 1.3 below the high-pressure limit.

From this, it is straightforward to predict the total yield of hydroxyacetone in the oxidation of propene. This will allow us to verify our theoretical results against the experimental measurements. Assuming that the rate constant for the reaction of the 1-hydroxy-2-propoxy radical with O_2 is comparable to that of the $(CH_3)_2CHO^\bullet + O_2$ reaction, i.e., $k_{13} = 1.5 \times 10^{-14}$ exp($-200/T$) cm^3 molecule^{-1} s^{-1},[35] we find a pseudo-first-order rate at 298 K and 0.2 atm partial pressure of O_2 of $k_{13}[O_2] = 3.8 \times 10^4$ s^{-1}. Under these conditions, reaction with O_2 is 650 times slower than thermal dissociation. Since 80% of the formed oxy radicals dissociate promptly, the predicted overall yield of hydroxyacetone is only 0.03%, negligible compared to the yield of dissociation products. The relative importance of the O_2 reaction 13 will increase with decreasing temperature. At 220 K and 0.2 atm partial pressure of O_2, the estimated rate of reaction 13 with O_2 is 4.0×10^4 s^{-1}, i.e., 9 times slower than thermal decomposition at a total pressure of 1 atm. At that temperature, we have a prompt dissociation fraction of 60%, which leads to an overall hydroxyacetone yield of 4%. For an O_2 partial pressure of 600 Torr, i.e., the highest value in the experiments, we predict about 12% hydroxyacetone, consistent with the experimental upper limit of 15%. None of these low-temperature predictions have been corrected for the loss of peroxy radicals by reactions with NO and NO_2 to form nitrates and peroxynitrates, respectively.

Finally, it is useful to represent the calculated k_{1atm} and k_∞ values for the thermal dissociation of 1-hydroxy-2-propoxy radicals at $T = 220-300$ K by formal Arrhenius expressions:

$$k_{1atm} = 3.6 \times 10^{12} \exp(-7.05 \text{ kcal mol}^{-1}/(RT)) \quad \text{s}^{-1}$$

$$k_\infty = 3.5 \times 10^{13} \exp(-7.91 \text{ kcal mol}^{-1}/(RT)) \quad \text{s}^{-1}$$

These expressions are based on the theoretical k values at only 220 and 298 K, but the ln(k) versus 1/T curvature should not be too large, since the Arrhenius activation energies E_a obtained do not differ much from the barrier height of 7.24 kcal mol^{-1}. The low Arrhenius A factor of 3.6×10^{12} at 1 atm is a result of the falloff behavior for this reaction; at 300 K, the reaction is a factor of 2.2 below the high-pressure limit, while at 220 K this is only a factor of 1.3. If the reaction had the same pressure dependence at both temperatures, a higher preexponential factor would be recovered, closer to the one for the high-pressure limit. For this reason also, whereas ln(k_∞) versus 1/T exhibits upward curvature (on account of $T(Q^\ddagger/Q)$), ln(k_{1atm}) vs 1/T shows downward curvature. The probable error of 0.5−1 kcal/mol on the DFT barrier height implies a possible k_{1atm} error of a factor of 2−5 at 298 K and a factor of 3−10 at 220 K. An estimate for E_a can also be obtained from the experimental upper limit of 15% for the hydroxyacetone yield at 220 K and 0.8 atm O_2 on the basis of the approximate rate of reaction 13. Assuming 50% oxy radicals thermalization and an A_{1atm} factor on the order of 10^{13} s^{-1}, it follows that E_a should be below ~8 kcal/mol, which is consistent with our theoretically derived E_a of ~7 kcal/mol. The Arrhenius parameters derived here for 1 atm differ markedly from those recently proposed by Atkinson ($A_{1atm} = 2 \times 10^{14}$, $E_a = 12.8$ kcal/mol),[9] which would lead to a ~75% yield of hydroxyacetone from propene oxidation at 220 K and 0.8 atm O_2, in disagreement with our observations. A large part of this discrepancy is related to the higher reaction enthalpy of 8 kcal/mol used by Atkinson, compared to the DFT endoergicity of 2 kcal/mol. A similar discrepancy was also observed for $HOCH_2CH_2O$ dissociation,[3,4] suggesting that the parameters in Atkinson's correlation do not give optimal results for β-hydroxyalkoxy decomposition.

Conclusions

The OH-initiated oxidation of propene under conditions relevant to the atmosphere has been shown, both experimentally and theoretically, to lead primarily to the production of CH_2O and CH_3CHO. Reaction of the β-hydroxypropylperoxy radicals with NO leads to the formation of chemically activated β-hydroxypropoxy radicals. Theoretical analysis of this reaction found that the majority of the oxy radicals (80% at 300 K and 1 atm; 75% at 220 K and 0.2 atm) dissociates "promptly" to yield CH_2O and CH_3CHO. Although this prediction could not be verified quantitatively, it is fully consistent with the observations. For the analogous ethene case, the experimental and theoretical prompt dissociation fractions were found to agree within 10% (absolute).[3,4]

Dissociation is also the predominant fate of the thermalized oxy radicals, even at the cold temperatures of the upper troposphere. The barrier to decomposition of the $HOCH_2CH(O^\bullet)CH_3$ radical obtained by B3LYP-DFT/6-31G** is only 7.2 kcal/mol. This is consistent with the finding that even at 220 K and 0.8 atm O_2 no hydroxyacetone could be observed. The error on the B3LYP-DFT/6-31G** barrier is expected to be 0.5−1 kcal/mol; similar deviations were also found in calculations for the ethoxy, isopropoxy, and β-hydroxyethoxy radicals, for which experimental values are available.[4] It must be emphasized that the intramolecular hydrogen bond of the most stable $HOCH_2CH(O^\bullet)CH_3$ rotamers persists during the C−C bond rupture, thus keeping the barrier low. Even "cold" β-hydroxypropoxy radicals, as formed in $HOCH_2CH(OO^\bullet)CH_3 + R'O_2$ reactions, are predicted to yield only marginal amounts of hydroxyacetone, with the highest yield of 4% at the lowest relevant temperature of 220 K and a total pressure of 0.2 atm.

Acknowledgment. This work was financially supported by the European Commission, the Belgian Fund for Scientific Research (FWO), and the Upper Atmosphere Research Program of the NASA Mission to Planet Earth. NCAR is sponsored by the National Science Foundation.

Supporting Information Available: Complete set of geometric parameters, vibrational wavenumbers, rotational constants, and a three-dimensional representation for all molecules and transition states discussed in the text. This material is available free of charge via the Internet at http://pubs.acs.org.

References and Notes

(1) Singh, H. B.; Zimmerman, P. R. Atmospheric distribution and sources of nonmethane hydrocarbons. In *Gaseous Pollutants: Characterization and Cycling*; Nriagu, J. O.; John Wiley: New York, 1992; pp 177−235.

(2) Atkinson, R. *J. Phys. Chem. Ref. Data* **1997,** *26*, 215.

(3) Orlando, J. J.; Tyndall, G. S.; Bilde, M.; Ferronato, C.; Wallington, T. J.; Vereecken, L.; Peeters, J. *J. Phys. Chem. A* **1998**, *102*, 8116.

(4) Vereecken, L.; Peeters, J. *J. Phys. Chem. A* **1999**, *103*, 1768.

(5) Wallington, T. J.; Hurley, M. D.; Fracheboud, J. M.; Orlando, J. J.; Tyndall, G. S.; Sehested, J.; Møgelberg, T. E.; Nielsen, O. J. *J. Phys. Chem.* **1996,** *100*, 18116.

(6) Møgelberg, T. E.; Sehested, J.; Tyndall, G. S.; Orlando, J. J.; Fracheboud, J.-M.; Wallington, T. J. *J. Phys. Chem. A* **1997**, *101*, 2828.

(7) Bilde, M.; Wallington, T. J.; Ferronato, C.; Orlando, J. J.; Tyndall, G. S.; Estupiñan, E.; Haberkorn, S. *J. Phys. Chem. A* **1998,** *102*, 1976.

(8) Peeters, J.; Boullart, W.; Van Hoeymissen, J. *Proceedings of EUROTRAC Symposium '94*; Borrell, P. M., et al., Eds.; SPB Academic Publishing: The Hague, 1994; pp 110−114.

(9) Atkinson, R. *Int. J. Chem. Kinet.* **1997**, *29*, 99.

(10) Niki, H.; Maker, P. D.; Savage, C. M.; Breitenbach, L. P. *J. Phys. Chem.* **1978,** *82*, 135.

(11) Wittig, C.; Nadler, I.; Reisler, H.; Noble, M.; Catanzarite, J.; Radhakrishnan, G. *J. Chem. Phys.* **1985,** *83*, 5581.

(12) Shetter, R. E.; Davidson, J. A.; Cantrell, C. A.; Calvert, J. G. *Rev. Sci. Instrum.* **1987,** *58*, 1427.

(13) Tyndall, G. S.; Orlando, J. J.; Calvert, J. G. *Environ. Sci. Technol.* **1995,** *28*, 202.

(14) Taylor, W. D.; Allston, T. D.; Moscato, M. J.; Fazekas, G. B.; Kozlowski, R.; Takacs, G. A. *Int. J. Chem. Kinet.* **1980,** *12*, 231.

(15) Niki, H.; Maker, P. D.; Savage, C. M.; Breitenbach, L. P. *Chem. Phys. Lett.* **1978,** *55*, 289.

(16) Becke, A. D. *J. Chem. Phys.* **1992**, *96*, 2115; **1992**, *97*, 9173; **1993**, *98*, 5648.

(17) Lee, C.; Yang, W.; Parr, R. G. *Phys. Rev. B* **1988**, *37*, 785.

(18) Scott, A. P.; Radom, L. *J. Phys. Chem.* **1996**, *100*, 16502.

(19) Hobza, P.; Sponer, J.; Reschel, T. *J. Comput. Chem.* **1995**, *16*, 1315.

(20) Kohn, W.; Becke, A. D.; Parr, R. G. *J. Phys. Chem.* **1996**, *100*, 12974.

(21) Van Duijneveldt, F. B.; Van Duijneveldt-van de Rijdt, C. M.; Van Lenthe, J. H. *Chem. Rev.* **1994**, *94*, 1873.

(22) Boys, S. F.; Bernardi, F. *Mol. Phys.* **1970**, *19*, 553.

(23) Frisch, M. J.; Trucks, G. W.; Schlegel, H. B.; Gill, P. M. W.; Johnson, B. G.; Robb, M. A.; Cheeseman, J. R.; Keith, T.; Petersson, G. A.; Montgomery, J. A.; Raghavachari, K.; Al-Laham, M. A.; Zakrzewski, V. G.; Ortiz, J. V.; Foresman, J. B.; Cioslowski, J.; Stefanov, B. B.; Nanayakkara, A.; Challacombe, M.; Peng, C. Y.; Ayala, P. Y.; Chen, W.; Wong, M. W.; Andres, J. L.; Replogle, E. S.; Gomperts, R.; Martin, R. L.; Fox, D. J.; Binkley, J. S.; Defrees, D. J.; Baker, J.; Stewart, J. P.; Head-Gordon, M.; Gonzalez, C.; Pople, J. A. *Gaussian 94*, revision E.2; Gaussian, Inc.: Pittsburgh, PA, 1995.

(24) O'Brien, J. M.; Czuba, E.; Hastie, D. R.; Fransisco, J. S.; Shepson, P. B. *J. Phys. Chem. A* **1998**, *102*, 8903.

(25) Peeters, J.; Boullart, W.; Pultau, V.; Vandenberk, S. *Proceedings of EUROTRAC Symposium '96*; Borrell, P. M., et al., Eds.; Computational Mechanics Publications: Southampton, 1996; pp 471−475.

(26) Vereecken, L.; Huyberechts, G.; Peeters, J. *J. Chem. Phys.* **1997**, *106*, 6564.

(27) Forst, W. *Theory of Unimolecular Reactions*; Academic Press: New York, 1973.

(28) Lightfoot, P. D.; Cox, R. A.; Crowley, J. N.; Destriau, M.; Hayman, G. D.; Jenkin, M. E.; Moortgat, G. K.; Zabel, F. *Atmos. Environ.* **1992**, *26A*, 1805.

(29) Jungkamp, T. P. W.; Smith, J. N.; Seinfeld, J. H. *J. Phys. Chem. A* **1997**, *101*, 1973.

(30) Stein, S. E.; Rabinovitch, B. S. *J. Phys. Chem.* **1973**, *58*, 2438.

(31) Troe, J. *J. Chem. Phys.* **1977**, *66*, 4745.

(32) Oref, I.; Tardy, D. C. *Chem. Rev.* **1990**, *90*, 1407.

(33) Cameron, D. R.; Borrajo, A. M. P.; Bennett, B. M.; Thatcher, G. R. J. *Can. J. Chem.* **1995**, *73*, 1627.

(34) Troe, J. *J. Chem. Phys.* **1977**, *66*, 4758; **1979**, *83*, 114.

(35) Atkinson, R.; Baulch, D. L.; Cox, R. A.; Hampson, R. F., Jr.; Kerr, J. A.; Troe, J. *Atmos. Environ.* **1992**, *26A*, 1187.